The Journal of Experimental Biology **199**, 1983–1997 (1996)
Printed in Great Britain © The Company of Biologists Limited 1996
JEB0317

MECHANICAL EFFICIENCY AND EFFICIENCY OF STORAGE AND RELEASE OF SERIES ELASTIC ENERGY IN SKELETAL MUSCLE DURING STRETCH–SHORTEN CYCLES

G. J. C. ETTEMA*
Department of Anatomical Sciences, The University of Queensland, Queensland 4072, Australia

Accepted 22 May 1996

Summary

The mechanical energy exchanges between components of a muscle–tendon complex, i.e. the contractile element (CE) and the series elastic element (SEE), and the environment during stretch–shorten cycles were examined. The efficiency of the storage and release of series elastic energy (SEE efficiency) and the overall mechanical efficiency of the rat gastrocnemius muscle (*N*=5) were determined for a range of stretch–shorten contractions. SEE efficiency was defined as elastic energy released to the environment divided by external work done upon the muscle–tendon complex plus internal work exchange from the CE to the SEE. Mechanical efficiency is external work done by the muscle–tendon complex divided by the external work done upon the muscle–tendon complex plus work done by the CE.

All stretch–shorten cycles were performed with a movement amplitude of 3 mm (6.7 % strain). Cycle frequency, duty factor and the onset of stimulation were altered for the different cycles. SEE efficiency varied from 0.02 to 0.85, mechanical efficiency from 0.43 to 0.92. SEE efficiency depended on the timing of stimulation and net muscle power in different ways. Mechanical efficiency was much more closely correlated with net power.

The timing of muscle relaxation was crucial for the effective release of elastic energy. Simulated *in vivo* contractions indicated that during rat locomotion the gastrocnemius may have a role other than that of effectively storing elastic energy and generating work.

Computer simulations showed that the amount of series elastic compliance can affect the internal energetics of a muscle contraction strongly without changing the muscle force generation dramatically.

Key words: rat, skeletal muscle, elasticity, energetics, work loop, locomotion, *Rattus norvegicus*.

Introduction

During locomotion, many muscles undergo so-called stretch–shorten cycles, during which the muscle is actively stretched prior to shortening (Hof *et al.* 1983). The work that is done upon the muscle during stretch can be stored in series elastic structures (mainly tendons) and subsequently re-utilised during shortening. Thus, during the shortening phase, when the muscle is generating mechanical work, an extra amount of (elastic) energy is released from the muscle–tendon unit. This energy is obtained from external sources (i.e. external with respect to the muscle–tendon unit, e.g. kinetic energy of the body, work done by antagonistic muscles) and would have been wasted if it had not been stored in the muscle–tendon system. Thus, the mechanism of storage and re-utilisation of elastic energy is an ‘energy-saving mechanism’ (e.g. Morgan *et al.* 1978; Biewener *et al.* 1981; Hof *et al.* 1983; Alexander, 1988).

It is well known that not all the work done on a muscle during stretch is stored in elastic form (e.g. Morgan *et al.* 1978; de Haan *et al.* 1989). Furthermore, not all the energy stored in elastic form may be re-utilised in an effective way (e.g. Hof *et al.* 1983; de Haan *et al.* 1989). However, little effort has been made to study in detail the efficiency of the process of storage and subsequent release of elastic energy under different loading conditions. In other words, how much of the energy that is stored in the series elastic structures is actually released to the environment rather than converted into heat internally? What factors play an important role in this process? The answers to these questions are important for understanding the impact that this energy-saving mechanism may have on the energetics of locomotion. To my knowledge, only Hof *et al.* (1983) have performed such an analysis for human calf muscles during walking. However, their results necessarily relied on rather crude estimates of series elastic compliance. Furthermore, they did not systematically investigate what the determining factors of effective storage and release of elastic energy were.

The issue of the efficiency of series elastic energy storage and re-utilisation is of interest for studies on the optimisation

*e-mail: g.ettema@mailbox.uq.oz.au.

of work output and metabolic efficiency using work loops, i.e. sinusoidal and *in-vivo*-like stretch–shortening cycles (e.g. Altringham and Johnston, 1990; Altringham and Young, 1991; Curtin and Woledge, 1993*a*,*b*; Barclay, 1994). Some of the work generated by the contractile element must be stored in the series elastic structures while muscle force rises during the onset of contraction. Thus, the process of storage and re-utilisation of elastic energy is also of importance for the efficiency of muscle contractions without any stretch period.

Hof *et al.* (1983) and Alexander (1988) proposed that the energy-saving mechanism operates optimally when all muscle–tendon shortening is accounted for by the series elastic structures. In other words, the length of the contractile element remains constant (concerted contraction, Hof *et al.* 1983). Thus, the contractile element would only have to utilise metabolic energy for force generation. Such a contraction probably does not provide the highest possible power output of the muscle–tendon unit. Ettema *et al.* (1990) have shown that, in stretch–shortening contractions, the release of series elastic energy may in fact hamper work production by the contractile element. Thus, there is some indication that optimal usage of series elastic energy and optimisation of contractile work may be incompatible.

The aim of this study is to examine the processes and efficiency of the storage and release of elastic energy in the muscle–tendon unit in detail, under a wide range of stretch–shorten cycles. The relationships between series elastic efficiency, mechanical efficiency and muscle power generation are examined to investigate the hypothesis that high net work production and net power are incompatible with the effective utilisation of large amounts of elastic energy.

Computer simulations were performed to assess the effects of different values of series elastic compliance on muscle performance.

Materials and methods

Experimental protocol

The experiments were performed on the medial head of the gastrocnemius of five male Wistar rats (body mass 325±22 g, mean ± S.D.). The gastrocnemius muscle mass was 0.87±0.08 g, muscle volume was 0.78±0.07 cm^3, muscle fibre length was 13.7±1.16 mm, and the length of the muscle–tendon complex was 44.7±1.5 mm (mean ± S.D.).

The main experimental protocol consisted of a series of five sinusoidal stretch–shorten cycles of 3 mm peak-to-peak amplitude (6.7 % strain at the level of the muscle–tendon complex) at optimum muscle length, i.e. the length at which maximal isometric force was generated. This amplitude is close to length changes of 7.3 % strain performed *in vivo* (G. J. C. Ettema, unpublished observation). During the middle three cycles, the muscle was supramaximally activated using 100 Hz stimulation bursts. The first and last cycle were performed passively to ensure that the muscle was acting well within the stretch–shorten movements during any period of activation, including the relaxation period.

Three parameters of the stretch–shorten cycle were varied, the cycle frequency, the timing of activation and the duty factor. Stretch–shorten frequencies of 3, 5 and 7 Hz were utilised at duty factors of 30 and 50 %. That is, the muscle was activated for 30 and 50 % of a complete stretch–shorten cycle. These parameter settings were chosen as they cover duty factors and stride frequencies during rat locomotion: *in vivo* gastrocnemius activity recorded using electromyography (EMG) is high for approximately 30 % of a stride and remains significant for approximately 50 % (Gruner *et al.* 1980), and stride frequencies range from less than 2 Hz (walk) to occasionally more than 7 Hz (gallop) (Cohen and Gans, 1975; Nicoloupoulos-Stournaras and Iles, 1984). To allow comparisons among the three cycle frequencies, the onset of activity was performed at pre-set radians of a cycle rather than at pre-set absolute times. The onset of activation occurred at −1.89, −1.26, −0.63, 0 and +0.63 rad, 0 rad being the top of a sine wave. In other words, an activation onset of 0 rad occurred at the muscle's peak length. The earliest onset of activation (−1.89 rad) corresponds to activation during 60 % of the stretch period. The onsets of activation at −1.26 and −0.63 rad seem to correspond with *in vivo* patterns (activation starts well before muscle peak length; Gruner *et al.* 1980). Fig. 1A describes the protocol for a 7 Hz cycle, 50 % duty factor and −1.89 rad stimulation onset. Only those combinations that are physiologically feasible were performed, i.e. cycles in which stimulation did not occur only during stretch and in which activation ceased during shortening (before the muscle reached its shortest length). Thus, the earliest onset of stimulation with a 30 % duty factor and the latest onset with a 50 % duty factor were excluded.

Additional contractions were performed at the 3 Hz cycle

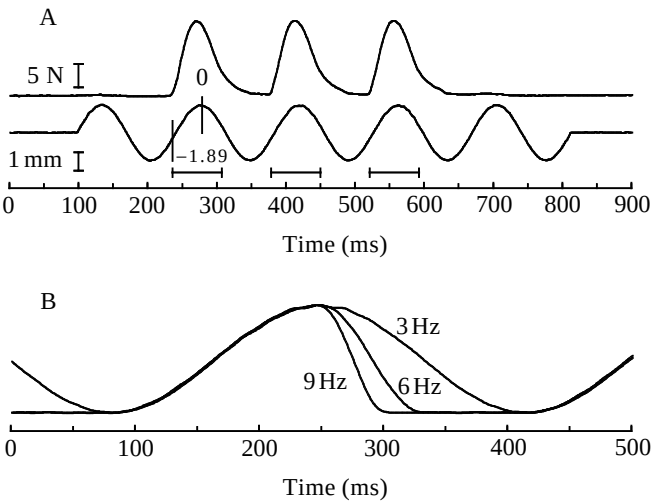

Fig. 1. (A) Experimental protocol for the main experiment. The lower trace is the enforced muscle–tendon length. Horizontal bars indicate periods of stimulation (in the diagram, the 7 Hz, 0.5 duty factor, −1.89 rad cycle is depicted). The top trace is the resulting muscle force. (B) Part of the enforced length traces of the 3 Hz cycle with different shortening frequencies. Absolute movement amplitude in A and B are the same (3 mm).

frequency. To simulate a ballistic shortening contraction, the shortening period of each cycle was performed at 6 and 9 Hz frequencies. The overall cycle frequency was maintained at 3 Hz by introducing an isometric period between the end of shortening and the next stretch (Fig. 1B). This experiment was performed at a 30 % duty factor, and −1.26 and −0.63 rad stimulation onsets. At 9 Hz shortening, the −0.63 rad stimulation onset was not performed as stimulation would end after the end of shortening.

An additional series of experiments was performed mimicking some aspects of *in vivo* loading of the rat gastrocnemius. Locomotion kinematics of the hindlimb and gastrocnemius activity patterns during running were derived from Gruner *et al.* (1980). The gastrocnemius length–time trace was determined by G. J. C. Ettema (unpublished data), who developed a geometrical model of the leg and calf muscle. Gruner *et al.* (1980) showed that the muscle activity was not constant over a cycle. A period of relatively high activity occurred over approximately 30 % of the entire cycle and started at around the time of first ground contact. However, a significant level of activity occurred for at least 50 % of the cycle. Thus, to investigate some of the effects of the timing of activation, the movement pattern was performed for six different stimulation protocols. The onset of activation started 0, 50, 100 and 150 ms after the onset of ground contact for a 180 ms duration (duty factor is 31 %). The 0 and 50 ms activation onsets were also performed with a 280 ms stimulation period (48 % duty factor). The pattern was performed at a 1.7 Hz cycle rate.

Surgery and equipment

The animals were anaesthetised with sodium pentobarbitone (Nembutal, initial dose 10 mg per 100 g body mass, intraperitoneally). The medial head of the gastrocnemius was freed from the surrounding tissues, leaving the blood supply intact. The sciatic nerve was severed, leaving a long distal nerve end attached to the muscle. The calcaneus was cut to leave a bony attachment at the Achilles tendon, which was used as an anchoring point for fixing the tendon to a metal wire. The wire was connected to the motor of a muscle puller, which was equipped with a strain gauge force transducer (accuracy to within ±0.05 N) and a linearly variable differential transformer (accuracy to within ±0.01 mm) in series with the muscle–tendon complex. The femur was scraped clean at the shaft so that it could be clamped onto the muscle puller fixation table. The position of this table was adjustable relative to the motor to set the initial muscle–tendon length (accuracy 0.02 mm).

The muscle was supramaximally activated by electrical stimulation of the severed nerve (100 Hz square-wave pulse train, 0.5 ms, 2 mA). The ambient muscle temperature was maintained at 30±0.1 °C with a purpose-built thermal controller. This temperature allows constant muscle conditions under the *in situ* situation and is still close to the *in vivo* temperature (33–35 °C; G. J. C. Ettema, unpublished observations). The muscle–tendon unit was covered with paraffin oil to prevent drying.

All movement and stimulation patterns were generated by computer. Force and muscle–tendon length traces were A/D-converted and sampled at a rate of 1000 Hz.

Mathematical model

The muscle–tendon unit was modelled as a contractile element (CE) and a series elastic element (SEE), aligned in series with each other (Ettema and Huijing, 1994*a*; see also Fig. 2B). The parallel elastic element was initially ignored as passive forces at the muscle lengths used in this study never exceeded 5 % of maximal isometric active force. The effects of this simplification are reported in the Results section. Furthermore, any viscous behaviour of the SEE was ignored as the literature suggests that the viscous effects are small (e.g. Hatze, 1981; van Ingen Schenau *et al.* 1988; Ettema, 1996*a*), which was confirmed in this study (see Results). Note that any actual viscous behaviour of the SEE is attributed to the CE.

When an element is lengthening, work is done upon it by the other element or by the environment. When an element is shortening, it does work (passively or actively) on the other element or on the environment. Any mechanical work done upon the contractile element is considered to be loss of energy as it cannot be converted into mechanical work by shortening of the contractile element. That is, the process is non-conservative (Hof *et al.* 1983; de Haan *et al.* 1989). This is irrespective of whether this work is done by the environment or originates from elastic energy in the series elastic structures. The energy that is stored in the series elastic structures during a stretch–shorten cycle has two sources. First, external work performed on the muscle can be directly stored in these structures when the muscle–tendon unit and the series elastic structures are stretched at the same time. Second, the contractile element can produce work, which is (temporarily) stored in the series elastic element when the CE is shortening and the SEE is lengthening.

To distinguish between the behaviour of the series elastic and contractile elements, the series elastic characteristics were determined according to Ettema and Huijing (1994*a*). Series elastic stiffness was determined by applying 210 Hz small-amplitude vibrations during the force plateau of tetanic contractions. The sample frequency for these stiffness measurements was 5000 Hz. The contractions were performed at different muscle lengths to vary isometric force levels. Thus, a force–stiffness relationship for the series elastic element was obtained. The data were fitted using a power function ($S=aF^b$), where S is stiffness and F is force. Mathematical integration of the converted force–compliance function ($C=S^{-1}=a^{-1}F^{-b}$), where C is compliance, yielded the force–elongation curve. Thus, from the muscle–tendon complex length–time and muscle force–time traces, it was possible to determine the length changes of series elastic and contractile elements at each moment during the stretch–shorten cycle. Numerical integration of muscle force over the length change of each element yielded the work done by or done upon each element at each moment. By comparing the work done by and done upon the entire muscle–tendon unit, series elastic element and contractile

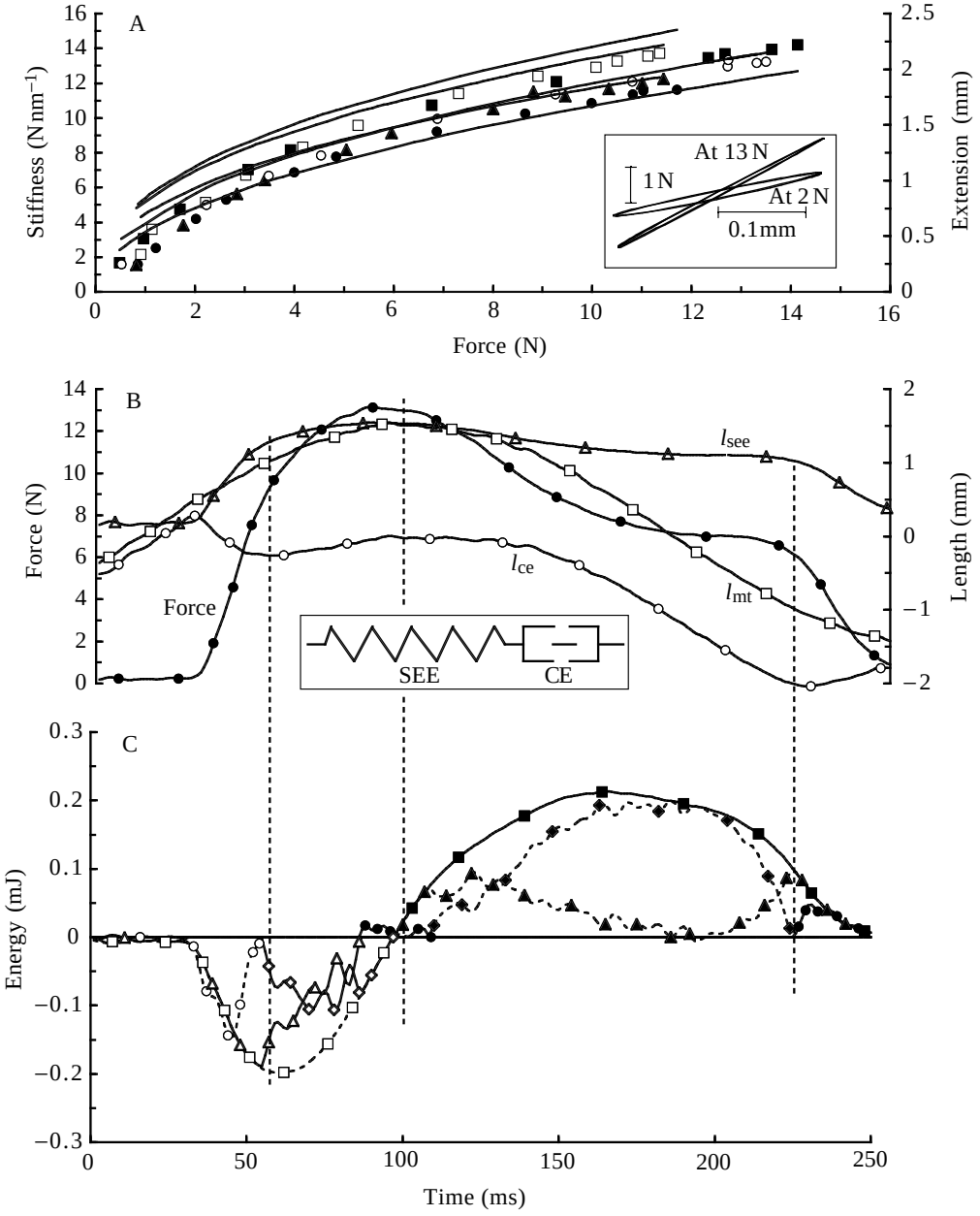

Fig. 2. (A) Series elastic element (SEE) stiffness plotted against force (different symbols indicate the five different muscles) and the calculated SEE extensions (lines). The inset shows two hysteresis loops obtained at mean forces of 13 N and 2 N. The area of the loop indicates the viscous loss of energy. For further explanation, see text. (B,C) Part of a stretch–shorten cycle (3 Hz, 0.5 duty factor, −1.26 rad stimulation onset) during which the muscle is activated. (B) Length of the muscle–tendon complex (l_{mt}, □), the contractile element (CE) (l_{ce}, ○), the SEE (l_{see}, △) and muscle force (●). The inset shows the model of the muscle–tendon complex used in the analysis. (C) Energy transfer (not cumulative over time) derived from force, l_{see}, l_{ce} and l_{mt} traces. Dashed line and □, external energy storage in the muscle–tendon complex; solid line and △, external energy storage in the SEE (part of dashed line and □); solid line and ◇, external energy storage in the CE (part of dashed line and □); dashed line and ○, internal energy storage in the SEE (from the CE); solid line and ●, internal energy release from the SEE (to the CE, i.e. internal energy loss); solid line and ■, external energy release from the muscle–tendon complex; dashed line and ▲, external energy release from the SEE (part of solid line and ■); dashed line and ◆, external energy release from the CE (part of solid line and ■; i.e. CE work directly transferred externally, without interference from the SEE). The vertical dashed lines indicate transition moments of energy flow (see also text).

element, the origin of energy storage by each element was identified. Fig. 2 shows an example of this analysis. Work exchange between the two elements of the muscle is referred to as internal exchange, and exchange of work between the muscle–tendon unit and the environment as external exchange. For each experiment, all work transfers were summed over the three stretch–shorten cycles and expressed as mean power (work rate) over the total duration of the activation periods.

The efficiency of the storage and release of series elastic energy (Eff_{see}) and mechanical efficiency (Eff_{mech}) was defined according to:

$$Eff_{see} = E_{see}^{+e}/(E_{ce}^{-e} + E_{see}^{-}), \quad (1)$$

and

$$Eff_{mech} = E_{mt}^{+e}/(E_{mt}^{-e} + E_{ce}^{+}), \quad (2)$$

where E is total work, and E^e is external work performed upon or done by the element in question. The + and – refer to work production and storage, respectively. The subscripts see, ce and mt refer to the series elastic element, contractile element and muscle–tendon unit, respectively.

Thus, SEE efficiency is defined as all external release of series elastic energy (to the environment) divided by all energy stored in the SEE plus the external work performed upon the contractile element. In other words, all work which is performed on the muscle–tendon system and the internal work produced by the CE that is subsequently stored in the SEE are accounted for. Note

that E_{ce}^{e} represents external work performed directly on the CE. Thus, this component is the amount of energy that is never stored in the SEE but is directly wasted by lengthening of the CE.

Mechanical efficiency is defined as all work produced by the muscle–tendon system (CE+SEE) divided by all external work performed on the muscle–tendon system plus all work produced by the CE.

Thus, the essential difference between the denominator of the Eff_{mech} equation and the Eff_{see} equation is that in the Eff_{see} definition work production by the CE that is performed directly on the environment (and not *via* the SEE) is not accounted for. Eff_{see} and Eff_{mech} refer to related but different processes. SEE efficiency is related to the exchange of energy to and from the SEE only, including energy storage (and loss) in the CE. Mechanical efficiency relates to the overall process of work storage and production by the muscle–tendon system, including contractile work released directly to the environment.

Simulation model of series elastic compliance

One experimental contraction (3 Hz movement, duty factor 0.3, stimulation phase −1.26 rad) was simulated using a two-element Hill-type muscle model consisting of a contractile element and a series elastic element (Ettema and Huijing, 1994*b*). The parallel elastic component was ignored as its behaviour was of no interest in this study. SEE and CE properties were derived from experimental data (Ettema, 1996*a*). The SEE stiffness–force curve was described by the same equation that was used to fit experimental force–stiffness data. In addition, a muscle with the experimentally determined force–stiffness curve (normal muscle), a muscle with a stiffness five times as high (stiff muscle) and a muscle with a threefold more compliant SEE (compliant muscle) were designed. The stiff muscle resembles the gastrocnemius in the absence of any tendinous structures (including aponeurosis), leaving only intracellular series elasticity (Ettema and Huijing, 1993). The compliant muscle approximately mimics a scaled gastrocnemius muscle of a wallaby, which is able to store approximately three times as much energy as can rat muscle in series elastic structures (Ettema, 1996*b*). CE length–force and force–velocity curves were fitted to the experimental data by means of a fourth-power polynomial and a hyperbolic function, respectively. The stimulation pulse train (100 Hz) was converted to an active state level using an exponential transformation and data from Hatze (1981).

Statistics

The effects of cycle frequency, duty factor and timing of activation on SEE efficiency were tested using analysis of variance (ANOVA) for repeated measures. The test was only performed on the parameter settings for which all combinations were performed (stimulation onset at −1.26, −0.63 and 0 rad). The effect of shortening speed was tested using a single-factor ANOVA. A *post-hoc* Tukey test was used to locate any effect.

Results

Fig. 2A shows the SEE force–stiffness data and calculated force–elongation curves for all five muscles. The maximum elongation varied to some extent among the muscles. However, the differences are mainly due to differences in the elongation at low forces (<0.5 N) where no stiffness measurements were obtained. Thus, the five force–elongation curves can be considered to be similar except for a vertical shift, which may be an artefact. This difference has negligible effects on the calculation of work production and energy storage as the extra elongation occurred at low force levels, i.e. with little energy involved (Ettema, 1996*b*). The maximum isometric force amounted to 13.07±1.19 N, or 214±16 kPa (mean ± S.D.).

In the inset of Fig. 2A, hysteresis loops for a 210 Hz vibration contraction at 13 N and 2 N are shown. The slope of the hysteresis loops gives the SEE stiffness values at the respective forces. Assuming that the hysteresis is caused by viscous behaviour of the series elastic structures, then the area of the loop indicates loss of elastic energy due to viscosity. It has been shown, however, that a considerable part of this hysteresis is actually due to small CE length changes during the vibrations, which are out of phase with the force trace and therefore do not affect the estimates of SEE stiffness from these hysteresis curves (Ettema, 1996*a*). The hysteresis is minimal at high force levels, i.e. when large amounts of energy are stored in the SEE, and increases with decreasing force. On the basis of the hysteresis loops over the measured force range, a theoretical maximal loss of SEE energy due to viscosity of 5 % was estimated. It should be noted, however, that these estimates of viscous energy loss apply to extremely high movement frequencies (210 Hz). Thus, during the work loop contractions, the viscous loss of elastic energy is likely to be less than 5 % of the total amount of series elastic energy. These estimates are within the order of magnitude found for a variety of isolated tendon preparations (energy dissipation ranging from 2.7 to 13.5 %, Bennett *et al.* 1986).

Fig. 2B,C shows a typical example of part of a sinusoidal stretch–shorten cycle. In Fig. 2B, the force and length traces are plotted. In Fig. 2C, the work transfers between the CE and the SEE and between the muscle–tendon complex and the environment are shown. In this particular example, the environment does work upon the muscle–tendon complex at the onset of contraction (open square symbols). All of this energy is stored in the SEE (open triangles), while the CE is shortening (see Fig. 2B) and does work upon the lengthening the SEE (open circles denote internal SEE energy storage). About half-way through the stretch period, the CE starts to stretch, together with the SEE, and thus external work is done upon the CE (open diamonds). Around the transition from muscle stretch to muscle shortening, a small amount of work is done on the CE by the SEE (filled circles denote internal SEE energy release). During muscle shortening, the muscle–tendon complex performs external work (filled squares), which partly originates from the SEE (filled triangles), but mainly from the CE (filled diamonds). At the

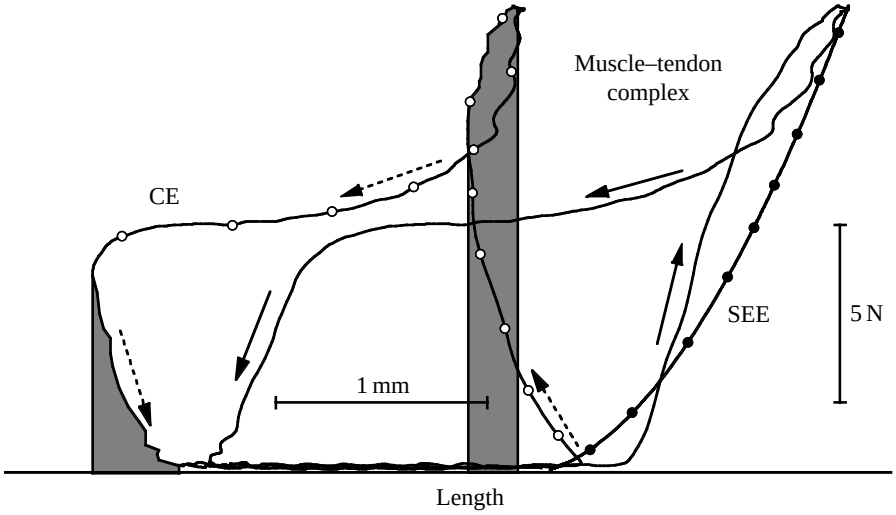

Fig. 3. The stretch–shorten contraction shown in Fig. 2 presented as a work loop (length–force tracing). The difference between the muscle–tendon and the contractile element (CE) (○) loops is accounted for by the series elastic element (SEE) length–force curve (●). Arrows indicate the direction of the loop. Shaded areas indicate the loss of mechanical energy by stretch of the contractile element, the right-hand area during muscle–tendon stretch and the left-hand area at the end of the shortening period during relaxation.

end of shortening, a substantial amount of series elastic energy is lost internally by stretching the CE (filled circles).

The elastic energy losses are clearly demonstrated in Fig. 3, which shows the work loop plots of the muscle–tendon complex and its elements for the contraction shown in Fig. 2. Although the general shape of the work loops of the muscle–tendon complex and the CE are similar, muscle–tendon complex and CE length changes do not coincide. When the muscle–tendon complex stretches, the CE may be shortening and *vice versa*. Whenever the CE is lengthening, work is lost as heat. Significant amounts of CE stretch occur in the late stretch phase and at the end of the shortening period (shaded areas).

Cycle frequency, duty factor and the timing of activation

Fig. 4 shows the results of the main experiment for stimulation onsets of −1.26, −0.63 and 0 rad. The ANOVA showed significant effects (P<0.01) for duty factor and stimulation onset on SEE efficiency (see Fig. 4A). Cycle frequency had no significant effect on SEE efficiency (P=0.084). SEE efficiency was generally higher for the 30 % than for the 50 % duty factor. The effect of the onset of stimulation depended strongly on the duty factor and cycle frequency. The same analysis for mechanical efficiency produced a different pattern (Fig. 4B). All three factors, including movement frequency, had a significant effect on mechanical efficiency. However, the differences in mechanical efficiency were less than for SEE efficiency: mechanical efficiency does not reach the very low levels shown for SEE efficiency.

Fig. 5 shows the results of all stretch–shorten cycles performed. Fig. 5A–C shows efficiency, net muscle power and

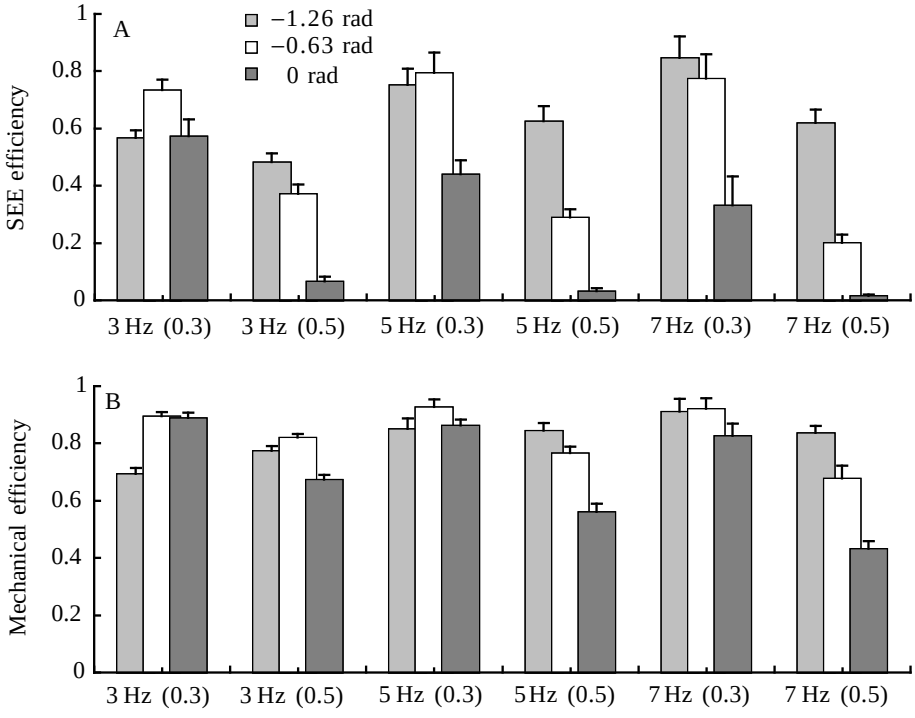

Fig. 4. Series elastic element (SEE) efficiency (A) and mechanical efficiency (B) for the stretch–shorten cycles used in the statistical analyses (ANOVA). The work loop frequency and duty factor (in parentheses) are given on the *x*-axis, the column shading indicates the stimulation onset (rad). Vertical bars indicate S.D. (N=5).

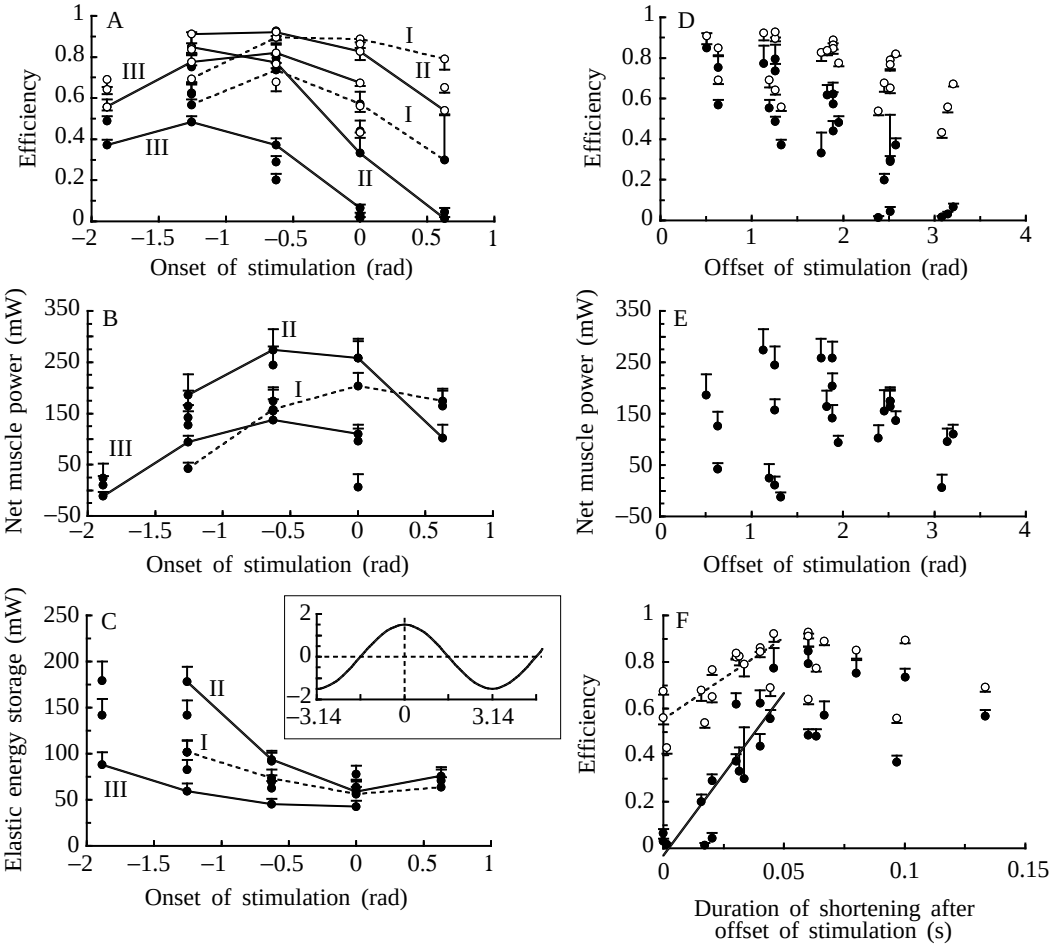

Fig. 5. (A) Efficiency (●, SEE efficiency; ○, mechanical efficiency), (B) net power and (C) series elastic energy (SEE) storage rate of all stretch–shorten cycles of the main protocol plotted against onset of stimulation. A power of 100 mW corresponds to a muscle mass-specific value of 115 W kg^{-1}. Note that power is calculated using the time of active periods only. Data connected by lines are from cycles similar except for stimulation onset. I, 3 Hz, 0.3 duty factor; II, 7 Hz, 0.3 duty factor; III, 3 Hz, 0.5 duty factor. (D) Efficiency and (E) power plotted against the offset of stimulation. (F) Efficiency as a function of time of shortening after stimulation was terminated. Solid and dashed lines are the regression lines for SEE efficiency and mechanical efficiency, respectively, for 0–0.05 s. Vertical bars indicate S.D. (N=5). Inset: relationship between muscle length (mm) and phase (rad) of the sinusoidal movement.

the series elastic energy exchange as a function of the onset of stimulation. Values connected by lines are for similar stretch–shorten cycles (same frequency and duty factor). Efficiency and muscle power show an inverted U-shaped curve when plotted against stimulation onset. However, the maximum values for SEE efficiency, mechanical efficiency and power do not all coincide. Maximal muscle power and maximal mechanical efficiency generally occur at a later stimulation onset than maximal SEE efficiency. The elastic energy exchange, i.e. the amount of energy stored in and released from the SEE, decreases when stimulation occurs later in the stretch–shorten cycle (Fig. 5C).

Despite their different relationships with stimulation onset, high efficiencies seem to concur with high values of net muscle power and series elastic energy exchange. Their interrelationships are shown in Fig. 6. There was no significant correlation between SEE efficiency and net muscle power, but the correlation between mechanical efficiency and net muscle power was high (Fig. 6A; r=0.761, P<0.001). Also, SEE efficiency and mechanical efficiency correlated strongly with each other (Fig. 6B; r=0.792, P<0.001). Muscle power did not show any correlation with the storage of series elastic energy (Fig. 6C) or with the actual externally utilised elastic energy (Fig. 6D). These results indicate that, although net muscle power and utilisation of series elastic energy may correlate to some extent, the mechanisms underlying the optimisation of these variables seem to be different.

Fig. 5D–F gives some indication of the mechanisms that dictate net muscle power and utilisation of series elastic energy. Fig. 5D,E shows efficiency and net muscle power as a function of the offset of stimulation. While no significant relationship exists between offset time and muscle power, SEE efficiency depends strongly on offset time (r=–0.854, P<0.001). Mechanical efficiency is also related to offset time, but to lesser extent (r=–0.493, P=0.014). This dependence can be explained by the loss of elastic energy at the end of shortening. When stimulation of the muscle ceases, it takes a certain amount of time before the muscle is totally relaxed and force has decreased to passive levels. Thus, to release elastic energy optimally to the environment during shortening, stimulation should end well before the end of shortening. To test whether the absolute time rather than the relative phase (rad) was a more important factor, efficiency was also plotted against the duration of shortening after the cessation of muscle activation (Fig. 5F). The correlation coefficient r was 0.669 (P<0.001) for SEE efficiency and not significant for mechanical efficiency (r=0.325, P=0.122). A strong relationship between efficiency and offset time only exists for the range 0–0.05 s of the non-stimulated shortening period (Fig. 5F, SEE efficiency: solid line, r=0.861, slope 14.0 s^{-1},

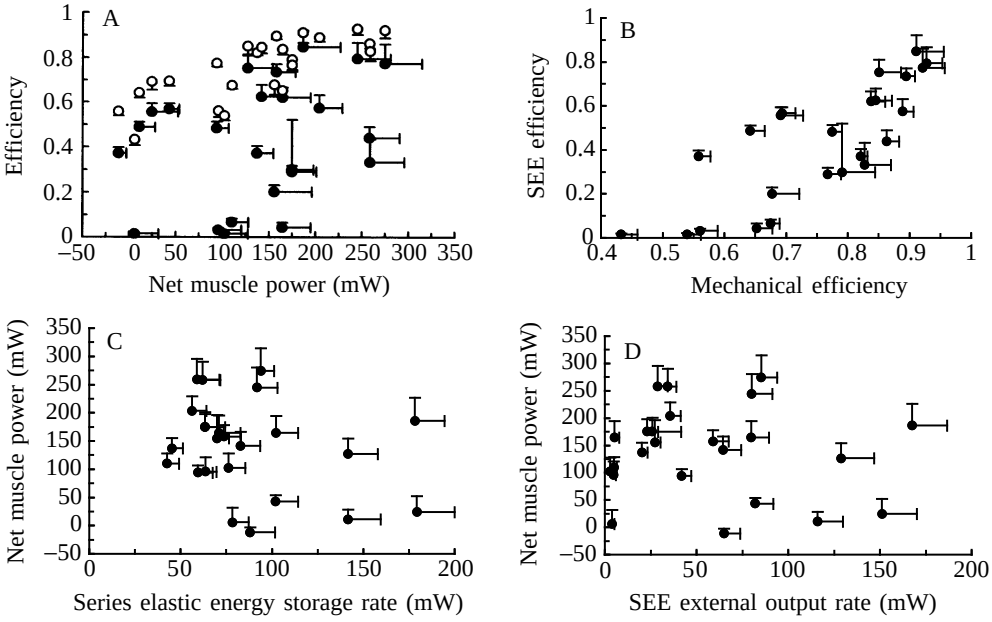

Fig. 6. Results shown Fig. 5 replotted as functions of each other (A–C) and of series elastic element (SEE) external power output (D), i.e. the part of SEE energy storage that is actually released externally. Horizontal and vertical bars indicate S.D. values (N=5). In A, ● is SEE efficiency; ○ is mechanical efficiency.

P<0.001; mechanical efficiency: dashed line, r=0.788, slope 7.0 s^{-1}, P<0.001).

Typical examples of work loops for the entire muscle–tendon unit as well as for the CE in six different stretch–shorten cycles are shown in Fig. 7.

Speed of shortening

Fig. 8 summarises the results from additional experiments in which the effect of shortening speed was investigated. The results for the 3 Hz shortening frequency are taken from the main experiment. An increased shortening speed did not enhance efficiency. In fact, a 6 Hz shortening frequency and an onset of stimulation at −0.63 rad resulted in a significantly lower SEE efficiency (ANOVA, Tukey *post-hoc* test). This low efficiency was caused by the insufficient time available for complete relaxation during shortening. Even though stimulation was terminated early in the shortening period, the muscle generated considerable force at the end of the brief shortening periods.

Mechanical efficiency showed a somewhat different pattern from SEE efficiency. The 3 Hz shortening frequency with early activation showed a significantly lower mechanical efficiency, whereas the efficiency at 3 Hz and late activation was significantly higher than the other values. At higher frequencies of shortening, the 6 Hz late-activation contraction showed a slightly increased efficiency compared with the other two contractions (6 Hz, −1.26 rad; 9 Hz, −1.26 rad). The striking difference between SEE efficiency and mechanical efficiency for the 6 Hz late-activation contraction is reflected in the highest net muscle power (179 mW *versus* 88–158 mW; 206 W kg^{-1} *versus* 101–182 W kg^{-1}) for this contraction. That is, this cycle is well designed for a high work output with a relatively high overall mechanical efficiency at the expense of an ineffective storage and release of series elastic energy.

Passive tension

In the model analysis described above, all energy stored in and released by the parallel elastic structures, i.e. work done by passive muscle tension, was implicitly attributed to the CE. To investigate the influence of passive force, the analysis of one muscle was repeated and corrected for passive muscle tension. This was carried out by fitting the passive force *versus* muscle length data during a number of passive cycles by an exponential function. The calculated passive force was then subtracted from total muscle force for all force traces prior to calculation of SEE and CE length changes and energy transfers. The results are compared with the original data in Fig. 9. The corrected efficiencies appear to be somewhat higher than the original values, without significantly changing any of the relationships mentioned above (the difference from the original efficiencies was less than 10 % of the original values).

In vivo *simulations*

For the assessment of the contractions simulating *in vivo* stretch–shorten cycles, it was necessary to correct the muscle force for passive tension. During the passive period (the *in vivo* swing phase), the muscle was stretched well beyond its optimum length (approximately 9 % of the muscle–tendon length), causing significant passive tension. The protocols are shown in Fig. 10A and numerical results are presented in Table 1.

Efficiency varied strongly with the stimulation protocol, reaching the highest values of 0.902 (SEE efficiency) and 0.968 (mechanical efficiency) at 30 % duty factor and late onset of stimulation (Fig. 10A,C). Very low efficiencies were found for the early onset of activation, at the moment of ground contact. In these work loops (I and V; Fig. 10A,B,D), much energy is absorbed by the CE during the stretch phase as well as during the last period of muscle shortening. Thus,

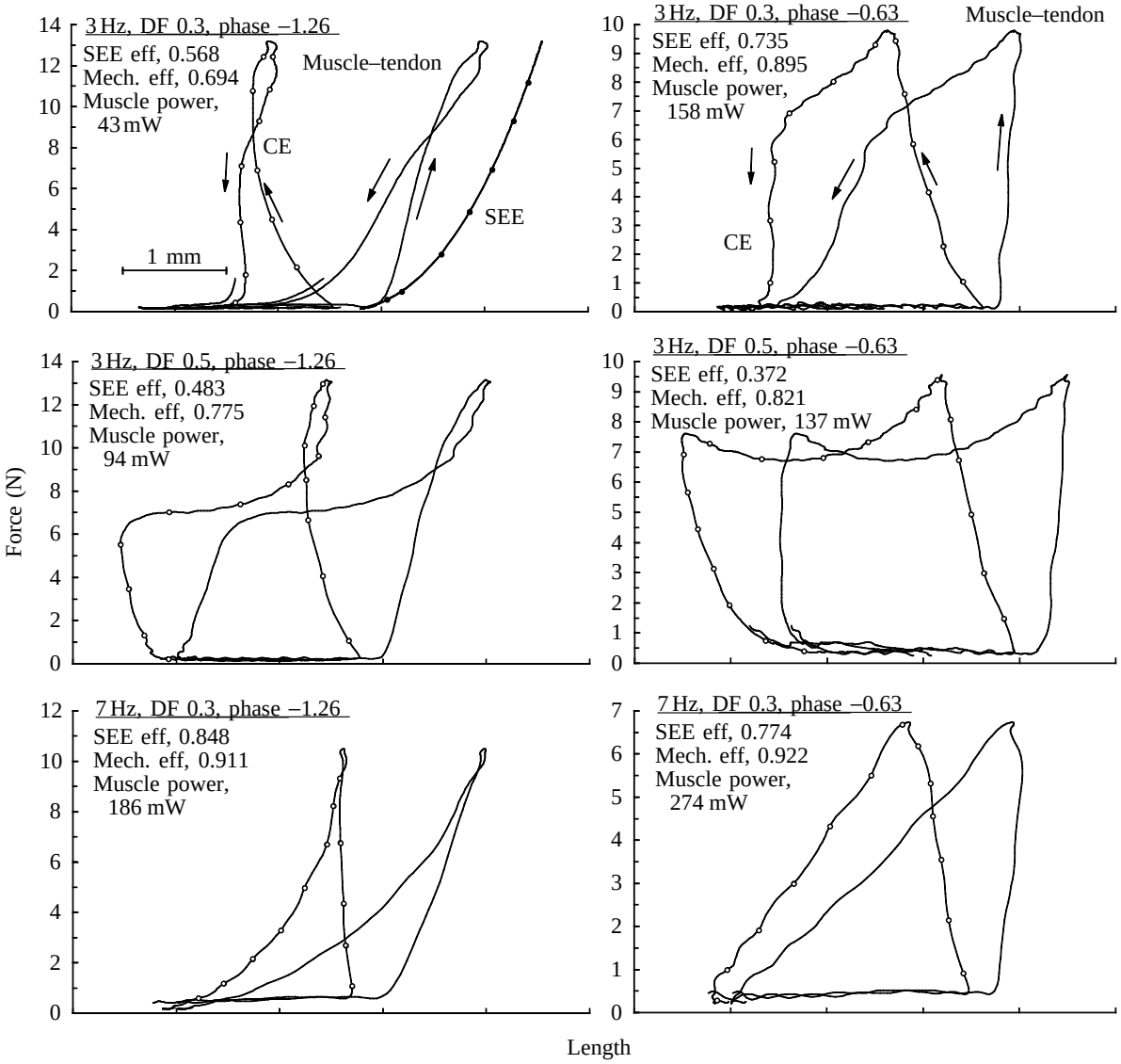

Fig. 7. Some examples of work loops from the main protocol. Line without markers, muscle–tendon complex; ●, series elastic element (SEE) (first diagram only); ○, contractile element (CE). Stretch–shorten cycle settings as well as the average efficiency and net power are indicated (N=5). In the upper diagrams, the direction of the loops is indicated; all others are counter-clockwise. The length scale is indicated in the top left-hand diagram. Mech. eff, mechanical efficiency; SEE eff, series elastic efficiency.

considering the muscle activity data of Gruner *et al.* (1980), it may be surprising to find that these work loops are the outcome of seemingly the most realistic stimulation protocols. However, note that the series elastic energy exchange and especially the amount of work done upon the muscle–tendon system were relatively high in these stretch–shorten cycles.

For the *in vivo* protocols, a high correlation was found between efficiency and net muscle power (SEE efficiency, r=0.767; P=0.075; mechanical efficiency, r=0.921, P=0.002).

SEE compliance simulation

Fig. 11 shows the results of the simulation of the

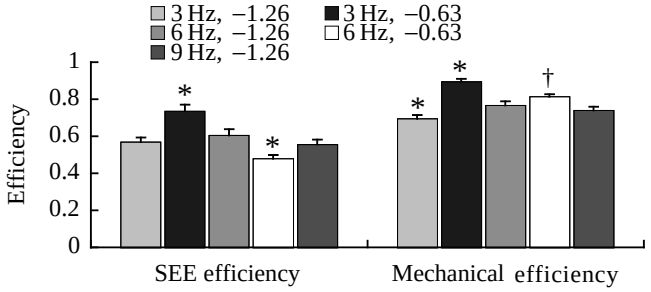

Fig. 8. Efficiency results from an additional experiment investigating the effects of frequency of shortening (3, 6 and 9 Hz). Shortening frequency and the onset of stimulation (in rad) are indicated. * indicates a significant difference from all other values; † indicates a significant difference from neighbouring values (*post-hoc* Tukey test, P<0.05). Values are means ± S.D. (N=5).

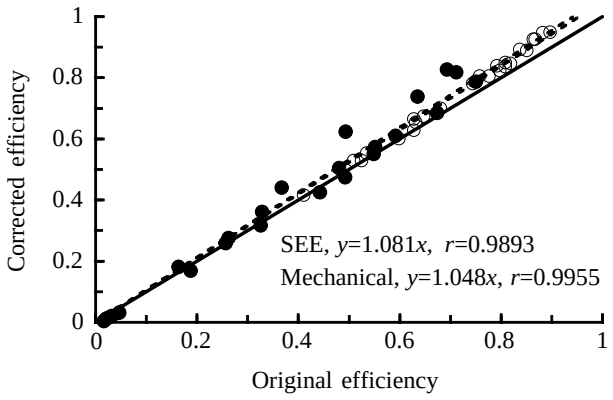

Fig. 9. Efficiency (●, SEE efficiency; ○, mechanical efficiency) for one muscle before (original values) and after (corrected values) correction for passive muscle force. The solid line is the line of identity; the dashed lines are the linear least-squares regression lines.

muscle–tendon units with three different series elastic compliances, stiff, normal and compliant. Fig. 11A shows the force traces. Note the delay in force build-up and the decrease in peak force with increased compliance. Furthermore, for the stiff muscle, a 100 Hz tremor in the force trace is apparent and is caused by the 100 Hz vibration of the active state. The active state vibration is the same for all three muscles, but it is not mechanically damped in the stiff muscle. Fig. 11B shows the muscle–tendon work loops. The normal and stiff muscles simulate the experimental results reasonably well (compare Fig. 7A with Fig. 11). The relatively small differences in the force tracings (Fig. 11A) between the normal and stiff muscle become more apparent when muscle behaviour is shown as a work loop (Fig. 11B,C). The amount of work done upon and released by the muscle, and particularly by the contractile element, differs considerably.

The compliant muscle behaves in a completely different

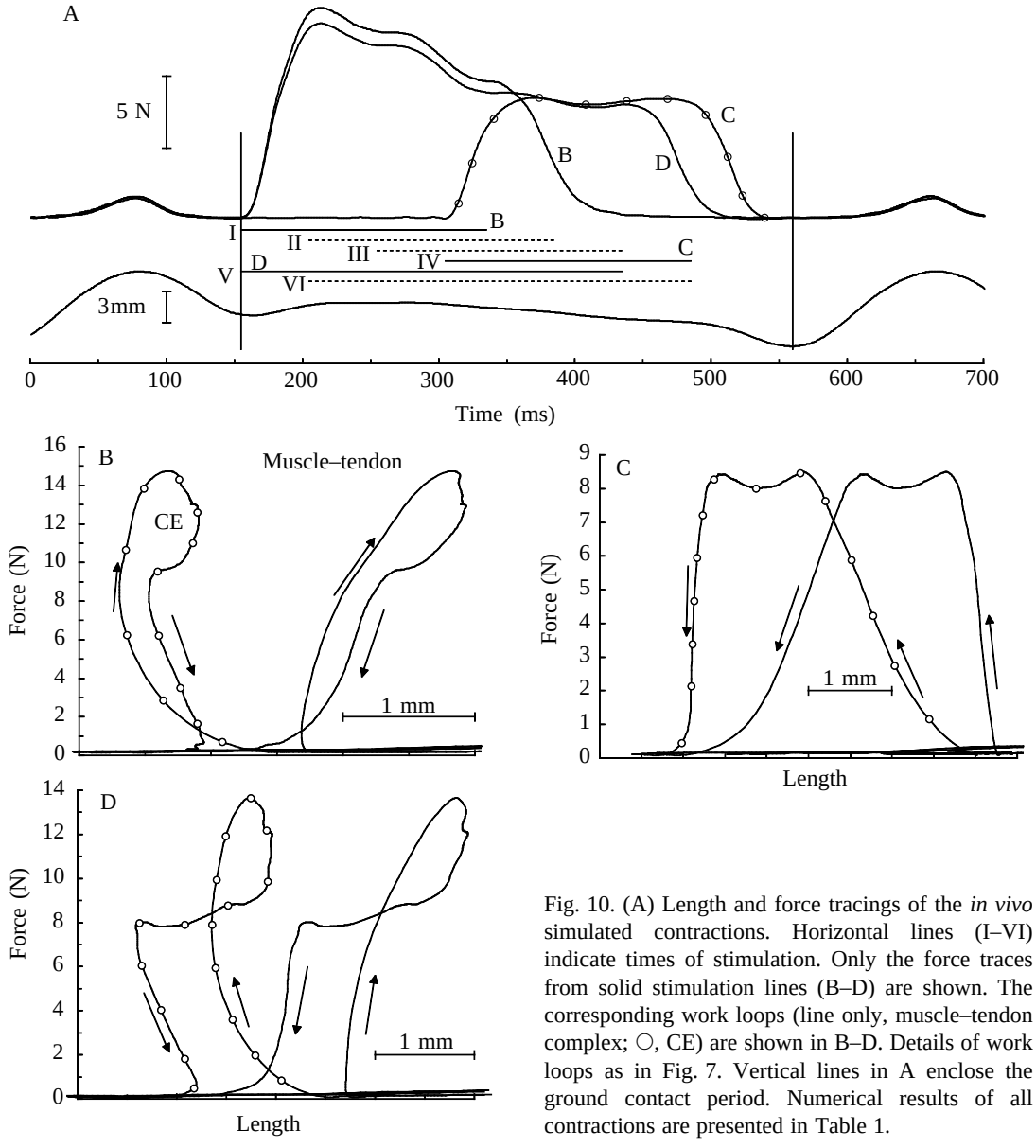

Fig. 10. (A) Length and force tracings of the *in vivo* simulated contractions. Horizontal lines (I–VI) indicate times of stimulation. Only the force traces from solid stimulation lines (B–D) are shown. The corresponding work loops (line only, muscle–tendon complex; ○, CE) are shown in B–D. Details of work loops as in Fig. 7. Vertical lines in A enclose the ground contact period. Numerical results of all contractions are presented in Table 1.

Table 1. *External and internal work exchange and efficiency for* in vivo *simulations and for three simulated muscle–tendon systems*

Simulation and model		Net muscle power (mW)	Muscle external work storage (mW)	*Loss* CE external work storage (mW)	CE work production (mW)	*Loss* SEE internal work release (mW)	SEE external work release (mW)	SEE total energy storage (mW)	SEE efficiency	Mechanical efficiency
In vivo simulations										
I	Fig. 10B	–19.1	95.6	52.0	58.0	24.9	34.0	58.9	0.306	0.498
		(1.8)	(6.3)	(2.0)	(7.6)	(5.9)	(2.5)	(7.7)	(0.013)	(0.008)
II		74.80	19.9	10.9	99.6	13.9	26.9	40.7	0.523	0.794
		(9.5)	(4.3)	(4.0)	(13.2)	(3.7)	(4.3)	(7.6)	(0.043)	(0.022)
III		92.29	8.0	5.0	116.7	19.3	16.6	35.9	0.404	0.806
		(11.7)	(2.0)	(1.1)	(14.6)	(4.6)	(5.1)	(8.5)	(0.064)	(0.031)
IV	Fig. 10C	111.33	5.7	4.9	115.4	0.9	34.0	33.2	0.902	0.968
		(14.1)	(3.7)	(3.5)	(15.3)	(1.7)	(7.1)	(7.0)	(0.060)	(0.018)
V	Fig. 10D	17.42	60.2	34.8	67.0	14.7	20.6	35.3	0.293	0.609
		(4.2)	(5.9)	(2.7)	(8.4)	(2.0)	(3.7)	(5.0)	(0.026)	(0.014)
VI		80.24	15.8	9.6	89.9	0.0	25.9	25.8	0.726	0.909
		(13.5)	(1.6)	(1.1)	(14.8)	(0.4)	(6.4)	(6.8)	(0.021)	(0.006)
SEE simulations										
Compliant		141.8	33.6	1.3	212.4	69.4	83.1	152.5	0.541	0.713
Normal		78.4	87.4	34.2	126.0	13.4	68.9	82.3	0.592	0.777
Stiff		30.9	116.6	100.7	135.1	3.4	14.2	17.6	0.120	0.586

CE, contractile element; SEE, series elastic element.

In vivo simulation protocols I–VI are shown in Fig. 10A. For all contractions, the same stretch–shorten movement was applied while altering the stimulation. N=5, except for protocols V and VI, N=4. S.D. is indicated in parentheses.

Muscle SEE simulations are based on experimental properties of the medial gastrocnemius of the rat (body mass 330 g). The series elastic force–stiffness curve is described by $S=aF^b$, where S is stiffness and F is force.

For all muscles, b=0.529. Compliant muscle, a=1.270; normal muscle, a=3.809; stiff muscle, a=19.043.

Two components of energy exchange are indicated by *Loss*, referring to wastage of mechanical energy by CE stretch. A power of 100 mW equals a muscle-mass specific power of 115 W kg^{-1}.

manner from the normal and stiff muscles. During muscle stretch, the contractile element produces work while shortening, whereas during a large part of the muscle shortening phase the contractile element is being stretched, wasting energy. Note that this occurs even though muscle force is reduced to zero before the end of muscle shortening. In other words, for optimal re-utilisation of elastic energy, it is not sufficient to reduce muscle force to low levels during muscle shortening.

Numerical results of the simulations are presented in Table 1. The compliant muscle generates the highest net muscle power, stores the least amount of external work, wastes large amounts of elastic energy internally, but generates most contractile work. This leads to a fairly low SEE efficiency, but a reasonably high overall mechanical efficiency. The stiff muscle produces little net power and takes up a large amount of external work (due to high peak forces), most of which is wasted by the contractile element. Work production by the contractile element is somewhat higher than for the normal muscle. This leads to a low SEE efficiency and a low mechanical efficiency.

Discussion

The stretch–shorten cycles performed in this study showed a concurrence of high muscle power and mechanical efficiency, whereas series elastic efficiency and the amount of elastic storage of energy were not related to net muscle power. Mechanical and SEE efficiency correlated strongly with each other. Thus, this study did not confirm the hypothesis that effective utilisation of high levels of series elastic energy is incompatible with high net muscle power. However, it was shown that effective utilisation of elastic energy and high net power do not depend on each other. This can be explained as follows. High net muscle power requires high power of the contractile element, i.e. internal work generation. High contractile power is hampered by a high level of series elastic energy exchange: the amount of contractile shortening is limited by shortening of series elastic structures (e.g. Avis *et al.* 1986; Ettema *et al.* 1990). However, the CE may generate work during muscle stretch that is stored in the SEE. During muscle shortening, this work can be released to the environment. Thus, net muscle power may be high when the

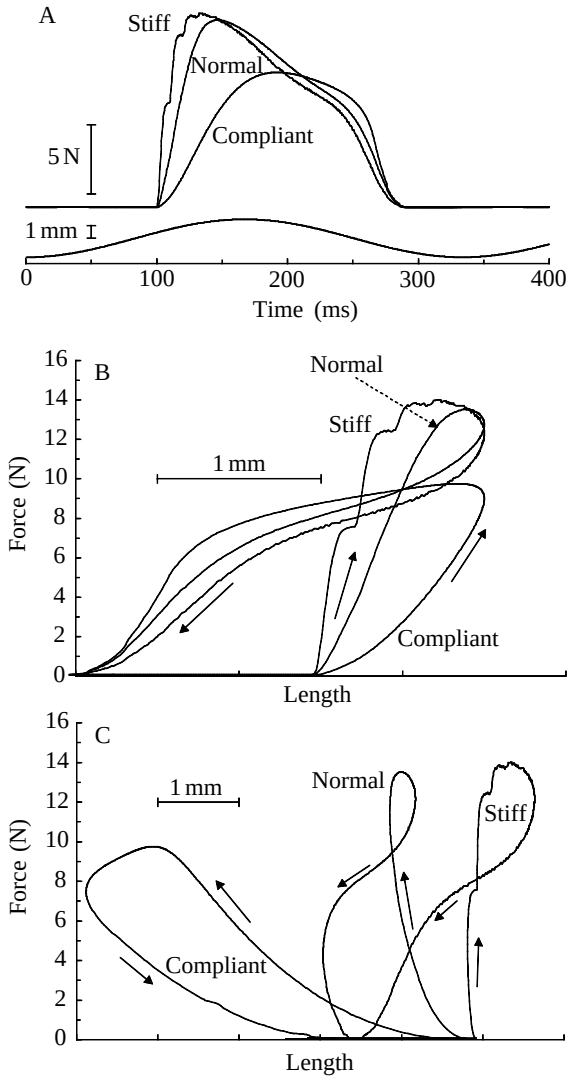

Fig. 11. Length and force tracings (A), muscle–tendon work loops (B) and contractile element (CE) work loops (C) of the series elastic element (SEE) computer simulations. Numerical results of all contractions are presented in Table 1.

SEE is effectively used to delay the release of CE work production to the environment. Yet, when much external energy is stored in the SEE during muscle stretch, the CE generates little or no work (CE lengthening is necessary to generate high force, a pre-requisite for high levels of series elastic energy). During the shortening subsequent to such a stretch, CE work production will normally be limited by the highly loaded SEE which will take up a significant amount of muscle–tendon shortening.

Why are mechanical and SEE efficiency strongly correlated with each other, while only mechanical efficiency correlates strongly with net muscle power? Mechanical efficiency has, almost by definition, a positive correlation with net muscle power [mechanical efficiency is equal to the ratio of positive muscle power (output) to negative muscle power (storage) plus CE power, whereas net muscle power equals positive muscle power minus the absolute value of negative muscle power]. However, if the series elastic energy exchange is relatively low, SEE efficiency is not important for the overall performance of the muscle. The high correlation between mechanical efficiency and SEE efficiency found over all contractions in this study was due to the impact of the experiments with high series elastic energy exchange. In these contractions, mechanical efficiency can only reach high levels if a significant part of the work transfer process, i.e. series elastic energy exchange, operates at high efficiency. However, this high correlation does not exclude the possibility of a reasonably high mechanical efficiency at a low series elastic efficiency (see Fig. 6B).

Shortening speed

For the optimal release of series elastic energy during shortening, it was hypothesised that ‘catapult’-like fast shortening would enhance the amount of external release of series elastic energy because of rapid force decay during shortening (e.g. Alexander and Bennet-Clark, 1977; Hof *et al.* 1983). However, the results of the fast shortening contractions did not confirm this hypothesis. In some cases, efficiency was even decreased (Fig. 8). The reason for this may be as follows. During fast shortening contractions, the time for the muscle to relax fully before the end of shortening is limited. Thus, especially with artificial supramaximal stimulation, it is extremely difficult to time the end of stimulation perfectly to fulfil two requirements. First, the force decay must be fast enough to reduce force to zero at the end of shortening. Second, the force decay must not occur too fast, as this would cause stretch of the contractile element during shortening. In other words, to obtain an optimal release of elastic energy, the contractile element must relax in such a way that it remains strong enough to maintain its length or even shorten, whereas it must relax sufficiently to allow a force reduction to zero at the end of shortening.

Fig. 5F indicates that, regarding SEE efficiency, the timing of relaxation becomes crucial within 50 ms of the end of shortening. At longer times, other factors apparently become more important for SEE efficiency. One of these factors is the amount of energy lost during muscle–tendon stretch. The relaxation time is affected by shortening speed (Edman, 1975), which is not accounted for in the present analysis. Thus, during faster shortening contractions, relaxation may start somewhat later than during slow shortening contractions to obtain a similar force decay rate.

The SEE as a lumped element

In the above analysis it is assumed that the lumped model of the series elastic structures (SEE) is valid for a partly activated (or relaxed) muscle. That is, all of the series elastic structures act as the same and single element when only part of the muscle fibre exerts force on it. This obviously cannot be the case for intracellular elastic structures, i.e. myofilaments and cross-bridge elasticity. However, for the extracellular structures, i.e. tendinous structures, forming the largest part of

the SEE of the rat gastrocnemius (Ettema and Huijing, 1993), this seems to be the case (Proske and Morgan, 1987). Furthermore, Ettema and Huijing (1994*b*) showed that the series elastic stiffness characteristics of rat gastrocnemius were not affected by the type of muscle activation (supra- or submaximal).

In vivo *muscle functioning*

As the stimulation protocols were artificial, the *in vivo* simulations performed in this study can only provide some indication of the utilisation of series elastic energy in the rat gastrocnemius muscle. The simulations indicate that mechanical efficiency may become close to 1.0 under *in vivo* conditions, i.e. perfect storage and release of elastic energy are possible. However, the physiologically most realistic contractions (I and V; Fig. 10A; Table 1) showed low efficiencies and low net power, yet storage of relatively high amounts of external work. Contraction I (30 % duty factor) also showed a high external, i.e. useful, release of series elastic energy. These results indicate that a muscle such as the gastrocnemius may function as a transfer system for energy between the knee and ankle rather than as a work generator, as was also found for the human gastrocnemius in jumping (Bobbert *et al.* 1986) and sprinting (Jacobs and van Ingen Schenau, 1992*a*). Furthermore, the gastrocnemius, as a bi-articular muscle, may perform important functions in motor control, i.e. directing push-off forces (Jacobs and van Ingen Schenau, 1992*b*), perhaps at the expense of its own mechanical efficiency.

As stated above, analysis of real *in vivo* muscle behaviour should be performed to elucidate the issue of the specific (energetic) function of a muscle (group) in locomotion. The challenge is to study different (mono- and bi-articular) muscles in a species, as well as species that display different locomotor behaviour patterns and apparently rely in different ways on the utilisation of elastic energy (e.g. Perry *et al.* 1988; Ettema, 1996*b*). Furthermore, a natural submaximal activation pattern is probably crucial for optimal muscle–tendon performance, as indicated earlier by Hof *et al.* (1983).

Work loop data in the literature can be interpreted to some extent in the context of the present study. Gregor *et al.* (1988) measured work loops of the cat soleus muscle. In all measurements shown (their Fig. 2), the muscle force shows a clear decay during shortening, a pre-requisite for effective re-utilisation of elastic energy. The *in vivo* work loop V (Fig. 10A) and the sinusoidal work loop (3 Hz, 0.5 duty factor, −1.26 rad; Fig. 7) of the present study are very similar in shape, and both had poor efficiencies. They also very closely resemble in shape one of the Gregor *et al*. (1988) work loops (their Fig. 2, cat 4, slow speed). It was reported that this cat demonstrated an awkward crouched gait (Gregor *et al.* 1988). Of course, this may be coincidental, but it would be interesting to investigate further this resemblance between work loops found under completely different conditions.

Griffiths (1989) reported work loops for the gastrocnemius of the wallaby during hopping. Griffiths' data (his Fig. 6) show work loops for which net work output is approximately zero. That is, the muscle works like an elastic spring, storing external energy and releasing the same amount externally. His data, however, do not indicate whether any energy is lost internally and compensated for by contractile work production. With the aid of data on the entire SEE compliance of the same species and muscle (Morgan *et al.* 1978), it can be deduced that, in net terms, most of the muscle–tendon length changes may have been taken up by the SEE. This still does not reveal how the CE length changed from moment to moment and, thus, how efficiently the energy-saving mechanism operated. Interestingly enough, the 'take-off' work loop in Griffiths' (1989) study shows a completely different pattern, with high net work production and little initial energy storage. This could be explained by the fact that the animal is accelerating from stance and thus has to increase its body's kinetic energy, i.e. generate contractile work, and cannot rely on the storage of elastic energy, which is simply not yet available. In this take-off work loop, muscle force decreased to zero by the end of shortening, indicating that SEE and mechanical efficiency may still be high.

Effects of altered SEE compliance

The SEE simulations give some indication about the importance of the SEE even for the rat gastrocnemius, a muscle that is not designed to store and utilise the very large amounts of elastic energy that are stored by the muscles of larger hopping mammals (Ettema, 1996*b*). By increasing series elastic stiffness fivefold (i.e. removing any tendinous tissue), the muscle force pattern does not alter dramatically (Fig. 11A). However, the energetics are greatly changed (Table 1). The stiff muscle stores far more external energy because of the rapid force rise during stretch. Most of this energy is lost, however, by stretch of the contractile element. Furthermore, the contractile element generates more work during shortening as it is not limited in its shortening by a shortening SEE. Still, net muscle power is low because of the poor elastic efficiency. In other words, the stiff muscle performs poorly in a mechanical sense. Of course, the 'stiff' muscle may show a very good performance at another work loop setting. The simulations merely indicate that, at a given muscle load (*in vivo* and *in situ*), even a relatively small amount of SEE compliance affects the muscle's (internal) performance greatly.

van Soest *et al.* (1995), in response to Baratta and Solomonow (1991), concluded that the insignificance of tendon compliance for mechanical performance in isometric contractions (Baratta and Solomonow, 1991) should not be generalised to contractions such as stretch–shorten cycles. The present study shows that such conclusions should be taken a step further: even if the mechanical effect (i.e. force response on activation) of series elastic compliance during stretch–shorten cycles is only small, it may well be that the internal performance, and thus probably the energetics, is greatly altered.

The highly compliant SEE muscle–tendon unit did not show

a particularly high mechanical efficiency. However, it allowed the CE to generate a large amount of work, which contradicts the results of Avis *et al.* (1986) and Ettema *et al.* (1990). The discrepancy lies in the fact that, in the simulation, most CE work is generated during stretch of the muscle and not during muscle shortening, the period on which these studies focused.

Efficiency

In this study, neither total energy input (work plus metabolism) nor total energy output (work plus heat) was measured. Thus, it was not possible to determine the overall efficiency of the contraction process during the stretch–shorten cycles. Obviously, SEE efficiency and mechanical efficiency are measures of parts of the total energy transfer process of muscle contraction. Thus, total efficiency must be lower than the efficiencies reported here. The most recent reports on maximal net efficiency of muscle contraction during sinusoidal work loops are approximately 0.3–0.4 for fast-twitch muscle (Curtin and Woledge, 1993*a*; Barclay, 1994) and approximately 0.5 for slow-twitch muscle (Curtin and Woledge, 1993*b*; Barclay, 1994). It would be very interesting to compare net efficiency with SEE efficiency and mechanical efficiency as defined in this study. Such a comparison would further elucidate the role of effective storage and re-utilisation of elastic energy for overall muscle performance.

References

ALEXANDER, R. MCN. (1988). *Elastic Mechanisms in Animal Movement*. Cambridge: Cambridge University Press.

ALEXANDER, R. MCN. AND BENNET-CLARK, H. C. (1977). Storage of elastic strain energy in muscle and other tissues. *Nature* **265**, 114–117.

ALTRINGHAM, J. D. AND JOHNSTON, I. A. (1990). Modelling muscle power output in a swimming fish. *J. exp. Biol.* **148**, 395–402.

ALTRINGHAM, J. D. AND YOUNG, I. S. (1991). Power output and the frequency of oscillatory work in mammalian diaphragm muscle: the effects of animal size. *J. exp. Biol.* **157**, 381–389.

AVIS, F. J., TOUSAINT, H. M., HUIJING, P. A. AND VAN INGEN SCHENAU, G. J. (1986). Positive work as a function of eccentric load in maximal leg extension movements. *Eur. J. appl. Physiol.* **55**, 562–568.

BARATTA, R. AND SOLOMONOW, M. (1991). The effect of tendon viscoelastic stiffness on the dynamic performance of isometric muscle. *J. Biomech.* **24**, 109–116.

BARCLAY, C. J. (1994). Efficiency of fast- and slow-twitch muscles of the mouse performing cyclic contractions. *J. exp. Biol.* **193**, 65–78.

BENNETT, M. B., KER, R. F., DIMERY, N. J. AND ALEXANDER, R. MCN. (1986). Mechanical properties of various mammalian tendons. *J. Zool., Lond.* **209**, 537–548.

BIEWENER, A., ALEXANDER, R. MCN. AND HEGLUND, N. C. (1981). Elastic energy storage in the hopping of kangaroo rat (*Dipodomys spectabilis*). *J. Zool., Lond.* **195**, 369–383.

BOBBERT, M. F., HUIJING, P. A. AND VAN INGEN SCHENAU, G. J. (1986). An estimation of power output and work done by the human triceps surae muscle–tendon complex in jumping. *J. Biomech.* **19**, 899–906.

COHEN, A. H. AND GANS, C. (1975). Muscle activity in rat locomotion: movement analysis and electromyography of the flexors and extensors of the elbow. *J. Morph.* **146**, 177–196.

CURTIN, N. A. AND WOLEDGE, R. C. (1993*a*). Efficiency of energy conversion during sinusoidal movement of white muscle fibres from the dogfish *Scyliorhinus canicula*. *J. exp. Biol.* **183**, 137–147.

CURTIN, N. A. AND WOLEDGE, R. C. (1993*b*). Efficiency of energy conversion during sinusoidal movement of red muscle fibres from the dogfish *Scyliorhinus canicula*. *J. exp. Biol.* **185**, 195–206.

DE HAAN, A., VAN INGEN SCHENAU, G. J., ETTEMA, G. J., HUIJING, P. A. AND LODDER, M. (1989). Efficiency of rat medial gastrocnemius muscle in contractions with and without an active prestretch. *J. exp. Biol.* **141**, 327–341.

EDMAN, K. A. P. (1975). Mechanical deactivation induced by active shortening in isolated muscle fibres of the frog. *J. Physiol., Lond.* **246**, 255–275.

ETTEMA, G. J. C. (1996*a*). Contractile behaviour in rat gastrocnemius muscle during small amplitude sine wave perturbations. *J. Biomech.* (in press).

ETTEMA, G. J. C. (1996*b*). Elastic and length–force characteristics of the gastrocnemius of the hopping mouse (*Notomys alexis*) and the rat (*Rattus norvegicus*). *J. exp. Biol.* **199**, 1277–1285.

ETTEMA, G. J. C. AND HUIJING, P. A. (1993). Series elastic properties of rat skeletal muscle: distinction of series elastic components and some implications. *Neth. J. Zool.* **43**, 306–325.

ETTEMA, G. J. C. AND HUIJING, P. A. (1994*a*). Frequency response of rat gastrocnemius medialis in small amplitude vibrations. *J. Biomech.* **27**, 1015–1022.

ETTEMA, G. J. C. AND HUIJING, P. A. (1994*b*). Skeletal muscle stiffness in static and dynamic contractions. *J. Biomech.* **27**, 1361–1368.

ETTEMA, G. J. C., VAN SOEST, A. J. AND HUIJING, P. A. (1990). The role of series elastic structures in prestretch-induced work enhancement during isotonic and isokinetic contractions. *J. exp. Biol.* **154**, 121–136.

GREGOR, R. J., ROY, R. R., WHITING, W. C., LOVELY, R. G., HODGSON, J. A. AND EDGERTON, V. R. (1988). Mechanical output of the cat soleus during treadmill locomotion: *in vivo* vs *in situ* characteristics. *J. Biomech.* **21**, 721–732.

GRIFFITHS, R. I. (1989). The mechanics of the medial gastrocnemius muscle in the freely hopping wallaby (*Thylogale billardierii*). *J. exp. Biol.* **147**, 439–456.

GRUNER, J. A., ALTMAN, J. AND SPIVACK, N. (1980). Effects of arrested cerebellar development on locomotion in the rat. *Exp. Brain Res.* **40**, 361–373.

HATZE, H. (1981). *Myocybernetic Control Models of Skeletal Muscle.* Pretoria: University of South Africa.

HOF, A. L., GEELEN, B. A. AND VAN DEN BERG, J. W. (1983). Calf muscle moment, work and efficiency in level walking; role of series elasticity. *J. Biomech.* **16**, 523–537.

JACOBS, R. AND VAN INGEN SCHENAU, G. J. (1992*a*). Intermuscular coordination in a sprint push-off. *J. Biomech.* **25**, 953–965.

JACOBS, R. AND VAN INGEN SCHENAU, G. J. (1992*b*). Control of an external force in leg extensions in humans. *J. Physiol., Lond.* **457**, 611–626.

MORGAN, D. L., PROSKE, U. AND WARREN, D. (1978). Measurements of muscle stiffness and the mechanism of elastic storage of energy in hopping kangaroos. *J. Physiol., Lond.* **282**, 253–261.

NICOLOUPOULOS-STOURNARAS, S. AND ILES, J. F. (1984). Hindlimb muscle activity during locomotion in the rat (*Rattus norvegicus*) (Rodentia: Muridae). *J. Zool., Lond.* **203**, 427–440.

PERRY, A. K., BLICKHAN, R., BIEWENER, A. A., HEGLUND, N. C. AND

TAYLOR, C. R. (1988). Preferred speeds in terrestrial vertebrates: are they equivalent? *J. exp. Biol.* **137**, 207–219.

PROSKE, U. AND MORGAN, D. L. (1987). Tendon stiffness: methods of measurement and significance for the control of movement. A review. *J. Biomech.* **20**, 75–82.

VAN INGEN SCHENAU, G. J., BOBBERT, M. F., ETTEMA, G. J., GRAAF, J. B. AND HUIJING, P. A. (1988). A simulation of rat EDL force output based on intrinsic muscle properties. *J. Biomech.* **21**, 815–824.

VAN SOEST, A. J., HUIJING, P. A. AND SOLOMONOW, M. (1995). The effect of tendon on muscle force in dynamic isometric contractions: a simulation study. *J. Biomech.* **28**, 801–807.